Title

Microcephaly Gene Links Trithorax and REST/NRSF to Control Neural Stem Cell Proliferation and Differentiation

Journal

Cell, 151(5)

ISSN

0092-8674

Authors

Yang, Yawei J
Baltus, Andrew E
Mathew, Rebecca S
et al.

Publication Date

2012-11-01

DOI

10.1016/j.cell.2012.10.043

Peer reviewed

Published in final edited form as:
Cell. 2012 November 21; 151(5): 1097–1112. doi:10.1016/j.cell.2012.10.043.

Microcephaly gene links Trithorax and REST/NRSF to control neural stem cell proliferation and differentiation

Yawei J. Yang[1,2,3,4,5,6], **Andrew E. Baltus**[1,2,4], **Rebecca S. Mathew**[4,7], **Elisabeth A. Murphy**[1,8], **Gilad D. Evrony**[1,2,3,4,6], **Dilenny M. Gonzalez**[1,2,4], **Estee P. Wang**[1,2,4,9], **Christine A. Marshall-Walker**[1,4], **Brenda J. Barry**[1,2,4], **Jernej Murn**[7,10], **Antonis Tatarakis**[7], **Muktar A. Mahajan**[11], **Herbert H. Samuels**[11], **Yang Shi**[7,10], **Jeffrey A. Golden**[12], **Muhammad Mahajnah**[13,§], **Ruthie Shenhav**[14,§], and **Christopher A. Walsh**[1,2,3,4,*]

[1]Division of Genetics, and Manton Center for Orphan Disease Research, Children's Hospital Boston, Boston, MA 02115, USA

[2]Broad Institute of MIT and Harvard, Cambridge, MA 02142, USA

[3]Program in Biological and Biomedical Sciences, Harvard Medical School, Boston, MA 02115, USA

[4]Howard Hughes Medical Institute

[5]Harvard-MIT Division of Health Sciences and Technology, Harvard Medical School, Boston, MA 02115, USA and MIT, Cambridge, MA 02142, USA

[6]Harvard MD-PhD MSTP Program, Harvard Medical School, Boston, MA 02115, USA

[7]Department of Cell Biology, Harvard Medical School, Boston, MA 02115, USA

[8]Department of Neuroscience, Northeastern University, Boston, MA 02115, USA

[9]Harvard School of Dental Medicine, Boston, MA 02115, USA; Current Address: Department of Orthodontics, University of Michigan, Ann Arbor, MI 48109, USA

[10]Division of Newborn Medicine, Children's Hospital Boston, Boston, MA 02115, USA

[11]Department of Pharmacology and Medicine, New York University, New York, NY 10016, USA

[12]Department of Pathology, Brigham and Women's Hospital, Boston, MA 02115, USA

[13]Child Development and Pediatric Neurology, Hillel Yaffe Medical Center, Hadera 38100, Israel, The Technion, Israel Institue of Technology, Haifa 32000, Israel

[14]Raphael Recanati Genetics Institue, Rabin Medical Center, Beilinson Campus, Petah Tikva 49100, Israel

SUMMARY

*Correspondence: christopher.walsh@childrens.harvard.edu, Mailing address: Christopher A. Walsh, MD, PhD, Room 15062, Center for Life Sciences, 3 Blackfan Circle, Boston, MA 02115, Phone: 617-919-2923, FAX: 617-919-2010.
§Authors contributed equally

SUPPLEMENTAL INFORMATION
Supplemental Information includes 7 figures, 7 tables, and Extended Experimental Procedures.

Microcephaly is a neurodevelopmental disorder causing significantly reduced cerebral cortex size. Many known microcephaly gene products localize to centrosomes, regulating cell fate and proliferation. Here, we identify and characterize a nuclear zinc finger protein, *ZNF335/NIF-1,* as a causative gene for severe microcephaly, small somatic size, and neonatal death. *Znf335*-null mice are embryonically lethal and conditional knockout leads to severely reduced cortical size. RNA-interference and postmortem human studies show that Znf335 is essential for neural progenitor self-renewal, neurogenesis, and neuronal differentiation. ZNF335 is a component of a vertebrate-specific, trithorax H3K4-methylation complex, directly regulating REST/NRSF, a master regulator of neural gene expression and cell fate, as well as other essential neural-specific genes. Our results reveal ZNF335 as an essential link between H3K4 complexes and REST/NRSF, and provide the first direct genetic evidence that this pathway regulates human neurogenesis and neuronal differentiation.

INTRODUCTION

Brain development requires carefully regulated yet continuously changing patterns of gene and protein expression. Cerebral cortical neurons are formed from progenitors that at the earliest stages divide mainly symmetrically to expand the progenitor population. At later stages, these apical progenitors divide increasingly in an asymmetrical fashion to produce one progenitor cell and a second, more differentiated cell, either a neuron, or a transit-amplifying progenitor cell that resides in the subventricular zone (Lui et al., 2011). Eventually, symmetrical divisions of progenitors are increasingly replaced by neurogenic cell divisions that produce the neurons of the cerebral cortex in an inside-first, outside-last sequence (Fietz and Huttner, 2011). Although much is known about the cellular patterns of neurogenesis, the molecular controls of this process remain relatively poorly understood.

Naturally occurring mutations of human cerebral cortical development have provided surprising genetic insights into the process of neurogenesis in vertebrates. Genetic causes of microcephaly implicate components of the mitotic spindle and proteins involved in DNA repair (Mahmood et al., 2011; Mochida, 2009; Thornton and Woods, 2009). However, human microcephaly genes have so far generally not highlighted the transcriptional pathways that animal studies implicate as essential to cerebral cortical neurogenesis (Molyneaux et al., 2007).

A key aspect of the regulation of gene expression during neurogenesis occurs at the level of chromatin structure. Acetylation, methylation, and phosphorylation of histone proteins affect the access of transcriptional proteins to DNA wrapped around nucleosomes (Bannister and Kouzarides, 2011), contributing to the complex control of gene expression. The Trithorax (TrxG) and Polycomb (PcG) chromatin remodeling complexes work in opposition to activate or silence gene expression, respectively (Ng and Gurdon, 2008). Recent studies shed light on the importance of chromatin regulatory complexes in brain development and developmental disease, although focus is placed mostly on PcG complex proteins and adult neurogenesis (Lessard and Crabtree, 2010; Ma et al., 2010). TrxG regulates developmental expression of many genes important for patterning, cell proliferation, and stem cell identity by maintaining genes in an active state (Fisher and Fisher, 2011). The TrxG complex activates gene expression through the methylation of Lysine 4 on histone H3 (H3K4) (Papp and Muller, 2006), a marker of actively transcribed genes or genes poised for transcription (Bernstein et al., 2005). SET1 methyltransferases (MLL1, MLL2, and SET1A/B) are the major enzymes carrying out H3K4 methylation, functioning in a multiprotein complex with Ash2L, WDR5, and RbBP5 (Schuettengruber et al., 2011). While TrxG has been implicated in Drosophila development (Paro et al., 1998), and while members of the complex have been implicated in vertebrate development and embryonic stem cells (Ang et al., 2011), the role

of TrxG has not been well studied in neural stem cells or human brain development (Schuettengruber et al., 2011).

Another critical epigenetic regulator of neurogenesis is the repressor element 1 (RE1)-silencing transcription factor (REST)/neuron-restrictive silencer factor (NRSF) (Chong et al., 1995; Schoenherr and Anderson, 1995). REST/NRSF acts as a transcriptional repressor through the recruitment of histone deacetylases (HDACs), which place chromatin in a condensed state via the removal of acetyl residues (Ballas et al., 2005). REST/NRSF is expressed in neural stem cells and is essential for maintaining progenitor cell fate by inhibiting neuronal specific genes (Sun et al., 2005). REST/NRSF has also been suggested to play roles in embryonic stem cells as well as mature cell types (Ballas et al., 2005; Johnson et al., 2008); however, the upstream regulation of REST/NRSF, as well as the interaction of REST/NRSF and TrxG, two central epigenetic regulators of neurogenesis, are unknown.

In this study, we identify a new regulator of vertebrate neurogenesis, *ZNF335*, in a family that presents with one of the most severe cases of microcephaly documented. Znf335 was previously cloned and identified as a co-regulator (NRC-Interacting Factor 1, Nif1) of nuclear hormone signaling (Garapaty et al., 2009), and as part of a complex containing components known to be involved in histone H3 methylation, but its functions have never been studied in vivo. We show that *ZNF335* is essential for normal brain development in human and mouse, and that ZNF335 interacts with a H3K4 chromatin methyltransferase complex. ChIP-PCR, ChIP-Seq, RNA-Seq, and microarray studies reveal that ZNF335 is essential for methylation and expression of brain-specific genes including the master progenitor regulator REST/NRSF. Knockdown of *ZNF335* disrupts progenitor cell proliferation, cell fate, and neuronal differentiation. Brain specific knockout leads to severely reduced to absent forebrain structure. Together, these data implicate a new microcephaly gene that coordinates global transcriptional regulation in brain development to affect cell fate, and defines an essential control system for REST/NRSF expression.

RESULTS

A new syndrome of profound microcephaly, neuronal degeneration, and neonatal death

A large consanguineous Arab Israeli pedigree presented with seven individuals (two of them identical twins) affected with one of the most severe cases of microcephaly (MCPH) seen to date (head circumference 9 standard deviations below mean), and death by one year of age in all but one case (Fig 1A–C). MRI at 3 months of age revealed extreme microcephaly with a severely simplified gyral pattern (Fig 1C). The cerebral cortex was even more notably smaller than the skull, with subarachnoid fluid separating the two, an indication of secondary shrinkage of the brain usually reflecting degeneration (Barkovich et al., 2007). Histopathology of Patient 5 at 7 months of age revealed a thinned cerebral cortex with only about 20% of the cortex showing the normal six cortical layers, and neuronal disorganization (Fig 1B). The few neurons that were present demonstrated little apparent polarity or dendritic maturation. Layer I, a normally cell-sparse layer containing many neuronal processes, was severely reduced in thickness, potentially reflecting defects in process outgrowth and/or defects of Layer I Cajal-Retzius cells. Layers II–VI, normally neuron-rich, showed sparse neurons of abnormally small size, suggesting incomplete neuronal differentiation. Well-differentiated pyramidal neurons, normally the most abundant neuron in the cortex, were also almost completely unidentifiable either because of aberrant differentiation, or severely reduced numbers (Fig 1B).

The cerebellum showed severely reduced external as well as internal granule cell layers (EGL, IGL)--which normally contain granule cell precursors and granule cells at this age

(Fig 1D)--suggesting widespread loss. There were few Purkinje cells, and increased numbers of eosinophilic, gemistocytic astrocytes in the Purkinje cell layer (PCL) consistent with a degenerative process. Calbindin immunoreactivity (Fig 1D) highlighted the severely reduced number, and abnormal localization and orientation of the rare remaining Purkinje cells (Fig 1D). A few mature granule cells persisted in the EGL (Fig 1E, Top), suggesting defective migration into the IGL. There is also a strikingly cell-sparse IGL, normally the location of countless mature granule cells (Fig 1E, Bottom), suggesting profound defects in generation and/or survival. These post-mortem histological studies suggest that the responsible gene has essential roles in normal neurogenesis, neuronal migration, neuronal polarity, as well as neuronal survival. The small birth weight, length, and other somatic features indicate that somatic size was affected, as well as brain size (Supplemental Experimental Procedures).

A splice donor/missense mutation of *ZNF335* causes severe microcephaly

The genetic mutation was identified by linkage mapping and gene sequencing (RNA-seq), and was confirmed and further characterized using mRNA-transcriptome sequencing. Mapping using single nucleotide polymorphism (SNP) arrays, followed by fine mapping, identified a single, ~2Mb interval that was homozygous and identical-by-descent in all affected pedigree members (Fig 2A), and in none of the unaffected individuals (multipoint logarithm of odds (LOD)=4.54). Sequence analysis of the 40 genes in the minimal linked region showed only one homozygous nonsynonymous change not already identified in dbSNP: a G to A transition at position 3332 of the coding sequence of the *ZNF335* gene. All affected individuals were homozygous for this mutation, all parents were heterozygous, and an unaffected sibling was wild type consistent with an autosomal recessive mode of inheritance (Fig 2A). This change was absent from 100 Middle Eastern control patients, 200 sequenced unaffected Arabic control exomes and 2500 European control exomes (NHLBI GO Exome Sequencing Project), confirming it is not a rare benign change. This c.3332g>a mutation results in a predicted change of Arg (CGC) at amino acid position 1111 of the ZNF335 protein to His (CAC) (Fig 2B). Moreover, the c.3332g>a transition is located at the final position of the splice donor site of exon 20, and a G at this position is highly conserved in mammalian splice donor sites (Cartegni et al., 2002).

Northern analysis and high-throughput RNA-seq from lymphocyte cell lines derived from an affected patient and a heterozygous parent confirmed that the c.3332g>a mutation disrupted normal splicing. Whereas a cell line from an unrelated individual showed a normal 5Kb transcript (Fig 2C), both affected patient and heterozygous carriers showed a larger transcript, absent in the control, suggesting that the c.3332g>a mutation produces a larger transcript with intron retention. Some normally-sized transcripts in homozygous mutant lymphocytes suggests that some normally-spliced RNA (albeit encoding a R1111H mutation) is still formed. RNA-seq of cytoplasmic RNA verified the *ZNF335* mutation, and also revealed abnormal *ZNF335* transcripts with inclusion of both the introns (introns 19, 20) flanking the mutation-containing exon (Fig 2D, S1A) at significantly higher levels than in control cells (p-value of 1.57*E-31).

Western analysis of homozygous patient cells showed severely reduced ZNF335 protein levels at the previously reported size of ~190kD (Fig 2F). The inclusion of introns 19 and 20 leads to a premature stop codon that could cause transcript degradation (Isken and Maquat, 2007). Yet, a small amount (≈16% of control) of full-length, R1111H-mutated protein is still formed, suggesting that some transcript splices normally (Fig 2F), although this mutated protein appears to be less stable (Data not shown). No larger protein or degraded protein products were detected in the heterozygous parent or affected patient. Evolutionary analysis of available Znf335 orthologues indicates that R1111 falls in the 13th zinc-finger domain (Fig 2E), which is absolutely conserved in all known Znf335 sequences (Fig S1B). Interestingly, no clear *ZNF335* orthologue can be identified outside of vertebrates. These

results are all consistent with the hypothesis that the identified mutation in *ZNF335* is the causative mutation in this family.

ZNF335 is essential for early embryonic mouse development

In order to confirm that Znf335 is essential in early brain development, we examined mice with engineered null Znf335 mutations and observed that homozygous loss of Znf335 leads to early embryonic lethality as early as embryonic day 7.5 (E7.5), (Fig 3A, S2A–C). This essential requirement of Znf335 suggests that the human R1111H mutation could be hypomorphic, since it results in some stable protein, albeit carrying a missense mutation. Examination of 100 individuals with varying degrees of microcephaly—though none as severe—showed no other patients with *ZNF335* mutations, suggesting that null *ZNF335* mutations in humans may also be lethal. Our data suggest that *ZNF335* is essential for normal human brain development and mouse development, and prompted us to examine its function.

The pattern and timing of ZNF335 expression are consistent with roles in neurogenesis, and potentially other processes as well. Northern analysis of adult (Fig S2A) and embryonic (Fig S2B) human tissues revealed widespread expression of *ZNF335*, including during embryonic brain development. Western analyses of mouse brain tissue show that Znf335 expression peaks at the height of cortical neurogenesis from E13-E15 (Fig 3C). To localize the expression of Znf335 in specific cell populations, heterozygous genetrap mice containing a β-galactosidase fusion reporter gene were stained histochemically. Znf335-lacZ was expressed in the developing forebrain and midbrain of E8.5 embryos (Fig 3B, 3D). Immunofluorescence analysis using antisera raised against Znf335 confirmed expression in the ventricular zone (VZ), subventricular zone (SVZ), as well as at lower levels in the developing cortical plate, but showed almost undetectable expression in NeuN-labeled neurons of the cortical plate at E12.5 and E14.5 (Fig 3D). At P10-P30, Znf335 expression returns at low levels in the adult cerebral cortex, hippocampus and cerebellum, possibly linked with neuronal maturation (Fig 3C, 3D, 3F, S2D, and data not shown). Higher magnification showed Znf335 immunoreactivity in nuclei of progenitor cells where it co-localizes with DAPI-stained DNA (Fig 3E), but largely or completely absent from heterochromatic foci. This expression pattern is consistent with roles of Znf335 in the progenitor cells prenatally and with possible roles in gene expression.

ZNF335 regulates neural progenitor self renewal and neurogenesis

The expression of Znf335 in progenitor cells along with the reduced brain size of patients hint at a role in regulating proliferation. In addition, lymphoblast cells lines from patients show decreased growth (Fig 4A) and the p.R1111H mutation leads to decreased ZNF335 binding with Ki-67, a component of a chromatin complex expressed in virtually all proliferating cells, and required for growth and survival (Fig S3A) (Garapaty et al., 2009; Zheng et al., 2006). To assess roles of Znf335 in progenitor proliferation directly, we selectively removed Znf335 from cerebral cortical progenitor cells by electroporating GFP-expressing plasmids that express either an shRNA against *Znf335* (shRNA-ZNF335, Fig S3B–C), or an shRNA containing silent mutations, making it unable to target *Znf335* (UT-Control). Electroporation was performed into cortical progenitor cells at E9.5 and E12.5. Targeted cells were selected upon dissociation using Fluorescent Activated Cell Sorting (FACS) 24 hours post electroporation, and the formation of proliferating reaggregate spheres was used to assess progenitor cell proliferation. Knockdown of ZNF335 in both E9.5 and E12.5 progenitors led to a decrease in reaggregate sphere formation (Fig 4B), confirming the role of Znf335 in progenitor cell proliferation and self-renewal.

In utero electroporation into developing cortices allowed targeting of cortical progenitor cells along the ventricular zone and follow-up studies in the native 3D architecture of the brain. 48 hours post electroporation, fewer Znf335-depleted cells were observed in the VZ (Fig 4C, 4E), and this phenotype could be rescued by WT Znf335 but not by Mutated Znf335 (Fig 4C, 4E, S3D). Bromodeoxyuridine (BrdU) pulse labeling experiments showed that this decrease reflected fewer progenitor cells undergoing DNA synthesis even 24 hours post knockdown (Fig 4F). A BrdU/Ki67 co-labeling experiment was performed to mark progenitor cells that either remained in the cell cycle (P Fraction), or exited the cell cycle (Q Fraction). By 48 hours post knockdown, a greater proportion of targeted progenitor cells exited the cell cycle as compared to UT-Control or wildtype (WT) unelectroporated controls (Fig 4D, 4G). Taken together, these data show Znf335 is essential for progenitor self-renewal by maintaining activity in the cell cycle and preventing premature cell cycle exit.

We confirmed the premature cell cycle exit of Znf335-depleted cells by allowing electroporated mice to develop until adulthood. A higher proportion of Znf335-depleted neurons occupied in deeper layers of the cortex (Fig 4H, 4I), consistent with early cell cycle exit, and fewer occupied more superficial layers, the location of later born neurons. Znf335-depleted neurons also exhibited abnormal cell fates. While most control neurons were Cux1-positive and FoxP1-negative (markers of Layers II–IV and III–V, respectively), knockdown neurons instead took on the identity of lower layer, earlier born neurons (Cux1-negative, FoxP1-positive) (Fig 5A, 5C). These data indicate that Znf335 deficiency leads to premature neuronal fate determination, which causes a depletion of dividing cells and is consistent with our patient phenotype of reduced cortical size and abnormal cortical layering.

ZNF335 also regulates neuronal morphogenesis and dendrite outgrowth

Further analysis of Znf335-depleted neurons demonstrates abnormal neuronal morphology reminiscent of the patient histology (Fig 1B, 1D). Knockdown cells at P0 showed abnormal cell orientation and radial glia (Fig 5B-a,b). By P6 and P8, knockdown neurons showed smaller cell bodies and lacked normal vertical apical dendritic process (Fig 5B-c–f). By P16, the dendritic outgrowth of knockdown cells was disorganized, abnormally oriented (Fig 5B-g,h), and only 25% of cells showed dendrites orientated perpendicular to the pial surface versus 95% in controls (Fig 5D). By adulthood, knockdown neurons showed disorganized branching, abnormal orientation, and signs of breakdown in dendrites (Fig 5B-i-n). WT-Znf335 but not Mut-Znf335 rescued the orientation phenotype, confirming the specificity of this phenotype and that the p.H1111R mutation is deficient but likely hypomorphic (Fig 5D). These phenotypes are reminiscent of the sparse neurons with reduced dendrites and abnormal orientation seen in patient histology studies. Microarray analysis of neurons with decreased ZNF335 expression showed decreased expression of genes important for brain development, such as neuron-specific transcription factors, dendritic branching and pruning genes, cell cycle and specific signaling factors, and neuronal specific microtubule binding partners (Fig S4), all of which could contribute to the neuronal and patient phenotypes.

ZNF335 interacts with a chromatin remodeling complex

In order to elucidate how loss of *ZNF335* could have such broad roles, we identified candidate interacting proteins immunoprecipitating (IP) FLAG-tagged ZNF335 in stable HeLAS3 cell lines as well as from endogenous E14.5 developing mouse brain lysates. Experiments utilizing IP followed by mass spectrometry (MS) and western verification revealed that ZNF335 pulls down members of a human H3K4 methyltransferase complex such as MLL, SETD1A, CFP1, ASH2, RbBP5, and WDR5, and that the complex components have histone H3 methylase activity (Fig 6A, Table S1), (Garapaty et al., 2009; Schuettengruber et al., 2011). Together, these proteins form a complex analogous to that of the TrxG complex in *Drosophila*, or the complex COMPASS (Complex Proteins Associated

with Set1) in *Saccharomyces cerevisiae*—both required for specific activation of gene expression (Schuettengruber et al., 2011). Knockdown of members of this methyltransferase complex cause stunted embryonic development and death, while WDR5 expression activates self-renewal genes in embryonic stem cells (Ang et al., 2011). The interaction of ZNF335 with a H3K4 methyltransferase complex presents an avenue for the regulation of many genes, consistent with the widespread effects in brain and other tissues upon ZNF335 loss.

ZNF335 regulates histone methylation and expression of specific genes

Chromatin IP followed by deep sequencing (ChIP-Seq) identified ZNF335-bound promoters representing possible ZNF335-regulated genes. ChIP-Seq was performed on developing mouse E14.5 lateral telencephalon with two separate antisera and two biological replicates. Znf335 peaks overlapped with promoter regions (Fig 6B–C) of a variety of genes; for example, genes that play roles in cell proliferation, somatic development, cell death, neuronal maturation, and signaling pathways, among others (Fig S5, Table S2). Since ZNF335 interacts in a methyltransferase complex, we looked at the methylation patterns of these ZNF335-bound promoters (Shen et al., 2012), and the peaks of ZNF335-binding overlapped with the H3K4 trimethylation (H3K4me3) peaks (Fig S5A). Similarly, in patients with decreased ZNF335, H3K4me3 marks at the promoters of Znf335 bound genes were also decreased, while control H3K27me3 marks were unchanged (Fig S5B). Finally, since H3K4me3 is linked with gene expression, RNA-seq data from the parents and patients with low H3K4me3 marks also showed decreased expression of these ZNF335 target genes (FigS5C, Table S2). Together, these data hint at a role of ZNF335 in a methyltransferase complex that is important for the H3K4trimethylation and ultimately the expression levels of a large variety of genes. GeneGO analysis performed on the genes identified through ChIP-Seq, microarrays, and RNA-seq data from patients showed that the genes affected by Znf335 were involved in a variety of pathways important for both somatic development as well as brain development (Table S3–6).

ZNF335 is upstream of REST/NRSF

Interestingly, we observed Znf335 bound to the promoter region of the known progenitor cell master regulator *REST/NRSF* (Fig 6B). A direct relationship between ZNF335 and expression of *REST/NRSF* is suggested by decreased TrxG complex binding and decreased H3K4me3 marks at the *REST/NRSF* promoter (Fig 6D–E), as well as decreased mRNA levels of *REST/NRSF* in *ZNF335* mutant patients (Fig 6E). Decreased *REST/NRSF* expression was seen upon ZNF335 knockdown of HeLA and Hek293 cells (Fig 6G), supporting a close, potentially direct, relationship. Conversely, expression of a dominant-negative REST (*DN-REST*)--which contains the DNA binding domain only (Chong et al., 1995; Schoenherr and Anderson, 1995)--as well as overexpression of *REST/NRSF,* did not significantly alter *ZNF335* expression (Fig 6H–I). Rescue experiments also showed that premature cell cycle exit and premature migrating neurons in the absence of ZNF335 could be rescued by REST, but not by DN-REST, which caused a phenotype similar to Znf335 deficiency (Fig 6J). These data, along with the promoter binding of REST/NRSF by Znf335, suggest direct regulation of REST/NRSF expression by ZNF335 (Fig 6I), and provide an avenue for abnormal neurogenesis secondary to abnormal REST/NRSF regulation.

Roles of ZNF335 in neuronal production and differentiation

Further analysis of Znf335-knockdown neurons showed stereotypical neuronal morphology (small cell bodies, dendrites, axons), but with a surprising loss of immunoreactivity for *D11Bwg0517e/Fox3*, or Neuronal nuclei (*NeuN*), an ubiquitous marker of all differentiated neurons (Dredge and Jensen, 2011) (Fig 7A, 7B, S6A), suggesting an apparent state of incomplete neuronal differentiation. This failure to express mature neuronal markers could reflect the abnormal premature neurogenesis caused by early progenitor cell cycle exit (Fig

4D), or—perhaps more likely—could reflect direct requirements for Znf335 in controlling gene expression in postmitotic neurons or in neuronal maturation and activity. The altered morphology (Fig 5B), and the arrested development (Fig 7A) exhibited by Znf335 knockdown neurons is reminiscent of the altered neuronal phenotype, cortical layers and cortical size seen in patients (Fig 1B, 1C).

Similar to Znf335-depleted cortical neurons, Znf335 knockdown in cerebellar granule cells produced abnormal cell migration, morphology, and differentiation. Znf335-deificient cerebellar granule cells showed migration arrest with decreased migration into the IGL (Fig S6B–C) recapitulating the human phenotype (Fig 1D–E). Microarray (Fig S4) and immunohistochemistry (Fig 7C–D) of Znf335-deificient cells showed decreased Mef2C expression, suggesting an arrest of normal transcriptional patterns. Our findings that knockdown of Znf335 led to increased cell death (Fig S6D) might suggest that this effect is mediated through Mef2c (Mao et al., 1999).

Finally, to confirm the essential role of Znf335 in cerebral cortical neurogenesis, we created a brain-specific, conditional knockout of Znf335 to bypass the embryonic lethality of a global knockout (Fig 3A). *Emx1-Cre* mediated removal of *Znf335* (Znf335 CKO) (Fig S7) produced a brain with an essentially absent cortex lacking all cortical neurons at sites of *Emx1* expression (Fig 7E–F) (Gorski et al., 2002), with a modest reduction in cortical size in heterozygotes compared to controls (Fig 7E). The lack of cortical plate and cortical neurons is in accordance with the essential role of Znf335 in progenitor cells and postmitotic neurons. The small brain phenotype of the Znf335 CKO further confirms that *Znf335* is responsible for the severe phenotype seen in our patients, and verifies *Znf335* as a new microcephaly gene essential for neurogenesis and differentiation.

DISCUSSION

Here we identify *ZNF335/NIF1* as a central regulator of mammalian neurogenesis and neuronal differentiation. A splice donor/missense mutation of *ZNF335* results in an extremely small brain in humans, and genetic ablation leads to early embryonic lethality in mice, while Emx1-Cre driven knockout leads to virtual absence of cortical structure. Loss of Znf335 causes premature cell cycle exit of progenitors, precociously depleting the progenitor pool. Znf335 is a part of a H3K4 methyltransferase complex and associates with the promoters of many key developmental genes to affect H3K4me3 as well as expression levels of target genes. A critical downstream target of Znf335 is REST/NRSF (master regulator of neurogenesis) representing a pathway critical for this neurogenetic function. Beyond its effects on progenitor cell proliferation, Znf335 also has essential effects on cell fate and cell morphology (and ultimately survival).

Despite the profound phenotype of *ZNF335* mutation in humans, the mutation we describe is almost certainly hypomorphic. Overexpression of the human mutation can only partially rescue Znf335 deficiency, and conditional ablation of Znf335 in mouse cortex results in loss of essentially the entire cortex. Thus, null mutations in ZNF335 in humans are presumably embryonically lethal as in mice, illustrating the utility of unusual, partial loss-of-function mutations in humans to elucidate essential early embryonic functions of such genes.

This study provides direct insight into the function of TrxG complex proteins in embryonic neurogenesis. The interaction of Znf335 with proteins of the H3K4 methyltransferase complex suggests roles for Znf335 in the regulation, targeting, or stability of the complex. Epigenetic regulation causes programming of gene expression, and specific histone methylation can further orchestrate gene regulation in a cell type and tissue dependent manner. Mutations in neural specific chromatin regulatory complexes, nBAF, have been

shown to affect proliferation and are linked with microcephaly (Hoyer et al., 2012). Thus, this interaction provides a potential parallel for the broad effects of the ZNF335 mutation on human patients, the large number of genes and developmental processes altered by *Znf335* knockdown, as well as the embryonic lethality in *Znf335*-null mice, especially since knockouts of other histone methyltransferases are also lethal embryonically (Glaser et al., 2009).

Loss of Znf335 alters expression levels of many key genes--including *DLX homeobox* genes (early brain development), *Neurogenin, Nfib, Olig1, Math1, REST/NRSF, Co-REST 2* (neurogenesis)--among many other genes important for dendritic branching, cell adhesion, and signaling. Changes in these genes could explain phenotypes seen in the patients and correlate with abnormal neurogenesis evident in mouse models and account for the virtual absence of cortical neurons in the Znf335 CKO. Genes whose expression changes upon *Znf335* deficiency could be primary targets of Znf335, or secondary targets of other regulatory genes downstream of Znf335 such as REST/NRSF, but revealing Znf335 as a critical regulator of gene expression essential for proper neuronal development.

Znf335 also regulates differentiation and gene transcription in postmitotic neurons. Znf335 deficiency blocks normal expression of ‘canonical’ neuronal marker genes such as NeuN and Mef2C, which could be either a secondary effect of premature and improper neurogenesis or may hint at a role of Znf335 in regulating cell identity, survival, and activity of mature neurons. ZNF335 regulates a variety of non- REST/NRSF targets that are important for the final stages of neuronal differentiation, such as genes regulating dendritic branching, and ion channels, which may suggest roles of ZNF335 in other neuron specific transcriptional complexes.

Genetic causes of microcephaly continue to grow in diversity, and include proteins involved in vesicle trafficking, mitotic spindle organization, and DNA repair (Thornton and Woods, 2009). Premature neuronal fate specification, with consequent loss of progenitor cells, could be a frequent cellular mechanism resulting in microcephaly (Lehtinen and Walsh, 2011). ZNF335 deficiency causes additional feature of neuronal degeneration, making it strikingly different, and more severe, than other microcephaly syndromes, which are typically compatible with postnatal survival and in many cases some intellectual function. Thus our data reveal *ZNF335* as a unique type of microcephaly gene, and provides evidence of a new upstream regulator of the balance between progenitor cell division and differentiation.

EXPERIMENTAL PROCEDURES

Human Patients

Peripheral blood samples were collected from patients and unaffected family members and mapping was performed using single nucleotide polymorphism (SNP) arrays and microsatellite markers to narrow down the boundaries of shared homozygosity. All coding exons were sequenced in the area of homozygosity on chromosome 20q13.2 to reveal the only homozygous coding mutation in the gene *ZNF335*. All human studies were reviewed and approved by the institutional review board of the Children’s Hospital, Boston, the Beth Israel Deaconess Medical Center and local institutions

Animals

Timed pregnant CD1, and Swiss Webster dams (Charles River Laboratories and Taconic). Genetrap 1 and 2 (AY0030 and XG241) (The Genetrap Consortium). Ex-Utero and In-Utero electroporations were performed on timed pregnant E9.5-E14.5 embryos. All animal experimentation was carried out under protocols approved by the IACUCs of Harvard Medical School and Children’s Hospital Boston.

Culture Systems

Primary cortical neurons were isolated from E14.5 mouse cells and dissociated by the Papain Dissociation System (Wothrington Biochem. Corp). Cells were grown on Poly-L-Ornithine coated plates (Sigma) in Neurobasal (Gibco) with 0.6% glucose, B27 (Gibco), N2 (Gibco), 1mM Penicillin, Streptomycin, L-glutamine, and transfected 1hr post plating. Primary granule neurons were isolated from P5 mouse pups and grown on Poly-L-Ornithine coated cover slips in Basal Medium, Eagle (Gibco), with 10% Calf Serum (Hyclone), 1mM penicillin, streptomycin, L-glutamine; 25mM KCl. Neurons were transfected 2 days post plating with calcium phosphate. All experiments were analyzed in a double blind manner using an unpaired T-test.

CO-IP/Mass Spectrometry

See Supplemental Materials & Methods

RNA-Sequencing

See Supplemental Materials & Methods

ChIP-Sequencing

ChIP-Seq was performed on E14.5 cortical tissue with antisera against ZNF335/NIF1 (Bethyl 797, 798A) antibody. 1–10 ng of ChIP DNA was used to prepare libraries sequenced at Elim Biopharmaceuticals, Inc. Peaks were identified by MACS and gene names were identified using custom Python scripts. All of the raw ChIP-seq data were deposited to NCBI's Gene Expression Omnibus (http://www.ncbi.nlm.nih.gov/geo/) (deposition number GSE36386). Functional characterization of genes was carried out according to the GO rules by Metacore (http://www.genego.com/genego_lp.php). See Supplemental Materials & Methods

Znf335 CKO

Floxed allele was generated in a mixed C57/Bl6 and 129B6 background that would lead the removal of the Znf335 promoter and exons 1&2. See supplemental Materials & Methods

Supplementary Material

Refer to Web version on PubMed Central for supplementary material.

Acknowledgments

We thank D. Moazed, M.E. Hatten, B. Ren, D.M. Ferrero, and members of the Walsh laboratory for helpful discussions; L. Shechtman for tissue, N. Dwyer for early mapping, G. Mandel for DN-REST construct, E.E. Govek for help with cerebellar slices, K.S. Krishnamoorthy for control MRIs, D.J. Tischfield, L.B. Hills, K.D. Atabay, P.P. Wang, D.G. Tierney, and J.M. Felie for technical assistance. This work was supported by a Stuart H.Q. & Victoria Quan Fellowship (Y.J.Y.); a NIH MSTP grant T32GM007753 (Y.J.Y. and G.D.E.); a NIH T32 HD007466 (A.E.B.); The Damon Runyon Cancer Research Foundation DRG-2042-10 (R.S.M.); HHMI Medical Research Fellows Program (E.P.W.); RO1 DK16636 (H.H.S.); NIH grants (GM058012, GM071004, and CA118487) (Y.S.); grants from the NINDS (RO1 NS032457 and R01 NS35129), and the Manton Center for Orphan Disease Research (C.A.W.). C.A.W. is an Investigator of the Howard Hughes Medical Institute. The content is solely the responsibility of the authors and does not necessarily represent the official views of the NINDS or the NIH.

References

Ang YS, Tsai SY, Lee DF, Monk J, Su J, Ratnakumar K, Ding J, Ge Y, Darr H, Chang B, et al. Wdr5 mediates self-renewal and reprogramming via the embryonic stem cell core transcriptional network. Cell. 2011; 145:183–197. [PubMed: 21477851]

Ballas N, Grunseich C, Lu DD, Speh JC, Mandel G. REST and its corepressors mediate plasticity of neuronal gene chromatin throughout neurogenesis. Cell. 2005; 121:645–657. [PubMed: 15907476]

Bannister AJ, Kouzarides T. Regulation of chromatin by histone modifications. Cell Res. 2011; 21:381–395. [PubMed: 21321607]

Barkovich, AJ.; Moore, KR.; Jones, BV.; Vezina, G.; Koch, BL.; Raybaud, C.; Grant, PE.; Blaser, SI.; Hedlund, GL.; Illner, A. Diagnostic Imaging: Pediatric Neuroradiology. 1. Salt Lake City, Utah: Amirsys- Elsevier; 2007.

Bernstein BE, Kamal M, Lindblad-Toh K, Bekiranov S, Bailey DK, Huebert DJ, McMahon S, Karlsson EK, Kulbokas EJ 3rd, Gingeras TR, et al. Genomic maps and comparative analysis of histone modifications in human and mouse. Cell. 2005; 120:169–181. [PubMed: 15680324]

Cartegni L, Chew SL, Krainer AR. Listening to silence and understanding nonsense: exonic mutations that affect splicing. Nat Rev Genet. 2002; 3:285–298. [PubMed: 11967553]

Chong JA, Tapia-Ramirez J, Kim S, Toledo-Aral JJ, Zheng Y, Boutros MC, Altshuller YM, Frohman MA, Kraner SD, Mandel G. REST: a mammalian silencer protein that restricts sodium channel gene expression to neurons. Cell. 1995; 80:949–957. [PubMed: 7697725]

Dredge BK, Jensen KB. NeuN/Rbfox3 nuclear and cytoplasmic isoforms differentially regulate alternative splicing and nonsense-mediated decay of Rbfox2. PLoS One. 2011; 6:e21585. [PubMed: 21747913]

Fietz SA, Huttner WB. Cortical progenitor expansion, self-renewal and neurogenesis-a polarized perspective. Curr Opin Neurobiol. 2011; 21:23–35. [PubMed: 21036598]

Fisher CL, Fisher AG. Chromatin states in pluripotent, differentiated, and reprogrammed cells. Curr Opin Genet Dev. 2011; 21:140–146. [PubMed: 21316216]

Garapaty S, Xu CF, Trojer P, Mahajan MA, Neubert TA, Samuels HH. Identification and characterization of a novel nuclear protein complex involved in nuclear hormone receptor-mediated gene regulation. J Biol Chem. 2009; 284:7542–7552. [PubMed: 19131338]

Glaser S, Lubitz S, Loveland KL, Ohbo K, Robb L, Schwenk F, Seibler J, Roellig D, Kranz A, Anastassiadis K, et al. The histone 3 lysine 4 methyltransferase, Mll2, is only required briefly in development and spermatogenesis. Epigenetics Chromatin. 2009; 2:5. [PubMed: 19348672]

Gorski JA, Talley T, Qiu M, Puelles L, Rubenstein JL, Jones KR. Cortical excitatory neurons and glia, but not GABAergic neurons, are produced in the Emx1-expressing lineage. J Neurosci. 2002; 22:6309–6314. [PubMed: 12151506]

Hoyer J, Ekici AB, Endele S, Popp B, Zweier C, Wiesener A, Wohlleber E, Dufke A, Rossier E, Petsch C, et al. Haploinsufficiency of ARID1B, a member of the SWI/SNF-a chromatin-remodeling complex, is a frequent cause of intellectual disability. Am J Hum Genet. 2012; 90:565–572. [PubMed: 22405089]

Isken O, Maquat LE. Quality control of eukaryotic mRNA: safeguarding cells from abnormal mRNA function. Genes Dev. 2007; 21:1833–1856. [PubMed: 17671086]

Johnson R, Teh CH, Kunarso G, Wong KY, Srinivasan G, Cooper ML, Volta M, Chan SS, Lipovich L, Pollard SM, et al. REST regulates distinct transcriptional networks in embryonic and neural stem cells. PLoS Biol. 2008; 6:e256. [PubMed: 18959480]

Lehtinen MK, Walsh CA. Neurogenesis at the brain-cerebrospinal fluid interface. Annual review of cell and developmental biology. 2011; 27:653–679.

Lessard JA, Crabtree GR. Chromatin regulatory mechanisms in pluripotency. Annu Rev Cell Dev Biol. 2010; 26:503–532. [PubMed: 20624054]

Lui JH, Hansen DV, Kriegstein AR. Development and evolution of the human neocortex. Cell. 2011; 146:18–36. [PubMed: 21729779]

Ma DK, Marchetto MC, Guo JU, Ming GL, Gage FH, Song H. Epigenetic choreographers of neurogenesis in the adult mammalian brain. Nat Neurosci. 2010; 13:1338–1344. [PubMed: 20975758]

Mahmood S, Ahmad W, Hassan MJ. Autosomal Recessive Primary Microcephaly (MCPH): clinical manifestations, genetic heterogeneity and mutation continuum. Orphanet J Rare Dis. 2011; 6:39. [PubMed: 21668957]

Mao Z, Bonni A, Xia F, Nadal-Vicens M, Greenberg ME. Neuronal activity-dependent cell survival mediated by transcription factor MEF2. Science. 1999; 286:785–790. [PubMed: 10531066]

Mochida GH. Genetics and biology of microcephaly and lissencephaly. Seminars in pediatric neurology. 2009; 16:120–126. [PubMed: 19778709]

Molyneaux BJ, Arlotta P, Menezes JR, Macklis JD. Neuronal subtype specification in the cerebral cortex. Nat Rev Neurosci. 2007; 8:427–437. [PubMed: 17514196]

Ng RK, Gurdon JB. Epigenetic inheritance of cell differentiation status. Cell Cycle. 2008; 7:1173–1177. [PubMed: 18418041]

Omichinski JG, Pedone PV, Felsenfeld G, Gronenborn AM, Clore GM. The solution structure of a specific GAGA factor-DNA complex reveals a modular binding mode. Nat Struct Biol. 1997; 4:122–132. [PubMed: 9033593]

Papp B, Muller J. Histone trimethylation and the maintenance of transcriptional ON and OFF states by trxG and PcG proteins. Genes Dev. 2006; 20:2041–2054. [PubMed: 16882982]

Paro R, Strutt H, Cavalli G. Heritable chromatin states induced by the Polycomb and trithorax group genes. Novart Fdn Symp. 1998; 214:51–61. discussion 61–56, 104–113.

Schoenherr CJ, Anderson DJ. Silencing is golden: negative regulation in the control of neuronal gene transcription. Curr Opin Neurobiol. 1995; 5:566–571. [PubMed: 8580707]

Schuettengruber B, Martinez AM, Iovino N, Cavalli G. Trithorax group proteins: switching genes on and keeping them active. Nat Rev Mol Cell Biol. 2011; 12:799–814. [PubMed: 22108599]

Shen Y, Yue F, McCleary DF, Ye Z, Edsall L, Kuan S, Wagner U, Dixon J, Lee L, Lobanenkov VV, et al. A map of the cis-regulatory sequences in the mouse genome. Nature. 2012; 488:116–120. [PubMed: 22763441]

Sun YM, Greenway DJ, Johnson R, Street M, Belyaev ND, Deuchars J, Bee T, Wilde S, Buckley NJ. Distinct profiles of REST interactions with its target genes at different stages of neuronal development. Mol Biol Cell. 2005; 16:5630–5638. [PubMed: 16195345]

Thornton GK, Woods CG. Primary microcephaly: do all roads lead to Rome? Trends Genet. 2009; 25:501–510. [PubMed: 19850369]

Zheng JN, Ma TX, Cao JY, Sun XQ, Chen JC, Li W, Wen RM, Sun YF, Pei DS. Knockdown of Ki-67 by small interfering RNA leads to inhibition of proliferation and induction of apoptosis in human renal carcinoma cells. Life Sci. 2006; 78:724–729. [PubMed: 16111722]

HIGHLIGHTS

- Mutation in *ZNF335*, an essential brain development gene, leads to severe microcephaly
- ZNF335 is essential for progenitor maintenance and prevents premature differentiation
- ZNF335 interacts with a H3K4 methyltransferase complex to regulate gene expression
- ZNF335 is upstream of REST/NRSF, a master regulator controlling key neuronal genes

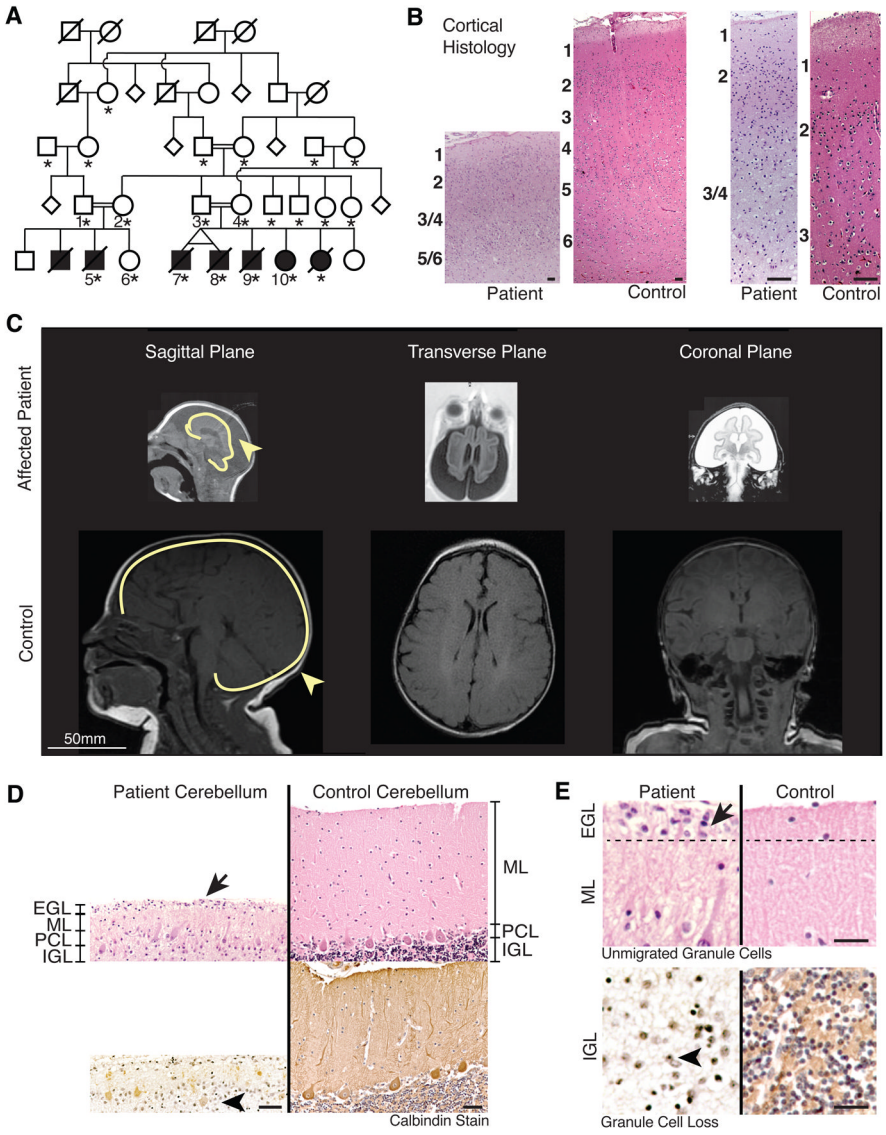

Figure 1. A new syndrome of severe microcephaly and neuronal degeneration

(A) Pedigree of family with severe microcephaly. Double lines: consanguineous marriages. Black shading: known affected. Diagonal line: deceased at time of publication. Asterisk (*): sequence analysis was completed on the individual.

(B) Cortical histology of patient vs. age-matched controls at 10X (left panels) and 40X (right panels) magnification. Patients show decreased cortical thickness and abnormal cortical layers. Scale: 300μm.

(C) MRI of patient vs. age-matched controls show decreased brain size including cerebellum and brain stem, increased extraaxial space, and enlarged ventricles. Whole brains are outlined in yellow, showing separation of brain from skull.

(D) Cerebellar histology. Calbindin-stained sections of patients vs. age-matched controls. Patients have persistent external granule cell layer (EGL), decreased molecular layer (ML), abnormal Purkinje cell layer (PCL), and decreased internal granule cell layer (IGL). Scale: 100μm.

(E) Patients have unmigrated EGL cells above a thinner molecular layer (top panels, arrow). Patients have severely reduced granule cell density compared to control (bottom panels, arrowhead). Scale: 50μm.
See also Supplemental Experimental Procedures.

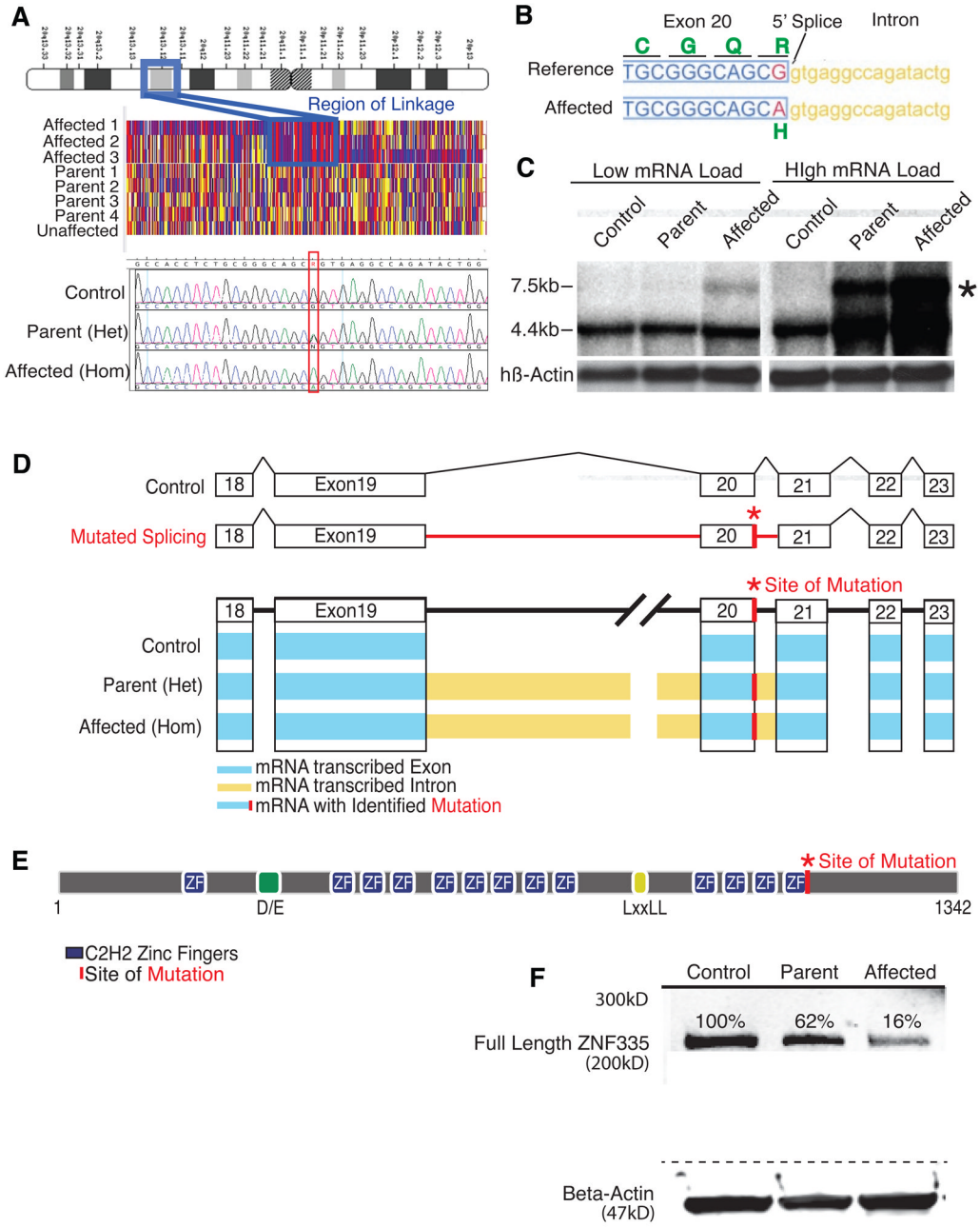

Figure 2. Severe microcephaly reflects a splicing/missense mutation *ZNF335*

(A) Patients show linkage at chromosome 20q13.12. Sequencing shows a c.3332g>a mutation in gene *ZNF335*. Upper panel: schematic of chromosome 20. Middle panel: single nucleotide polymorphism genotyping. Each column represents a SNP, and the red and blue indicate homozygosity, whereas yellow shows heterozygosity. A large region (boxed) shows mainly red and blue SNPs in affected patients with heterozygosity in parents. Bottom panel: representative sequencing data.

(B) Mutation is at 5′ Splice site of ZNF335 and leads to R1111>H missense mutation.

(C) Northern blot shows production of a new larger transcript (*) in heterozygous parents and homozygous patients.

(D) Schematic of exons and intronic splicing for a control and the predicted problems with intronic splicing in a patient with a c.3332g>a mutation. Schematic of RNA-sequencing data shows detection of reads within exons (blue), and within introns (yellow) upstream and downstream of the mutation-containing exon. Incomplete splicing is present in heterozygous parents and homozygous patients but not in control cells. RNA-sequencing data also detected the base change mutation (*).
(E) Predicted structure of ZNF335. Mutation lies in the last zinc finger motif.
(F) Western blot of patient lymphoblast cell lines show heterozygous parents and homozygous patients produce a reduced amount of full length ZNF335 protein, and no evidence of larger or degraded protein products.
See also Fig S1.

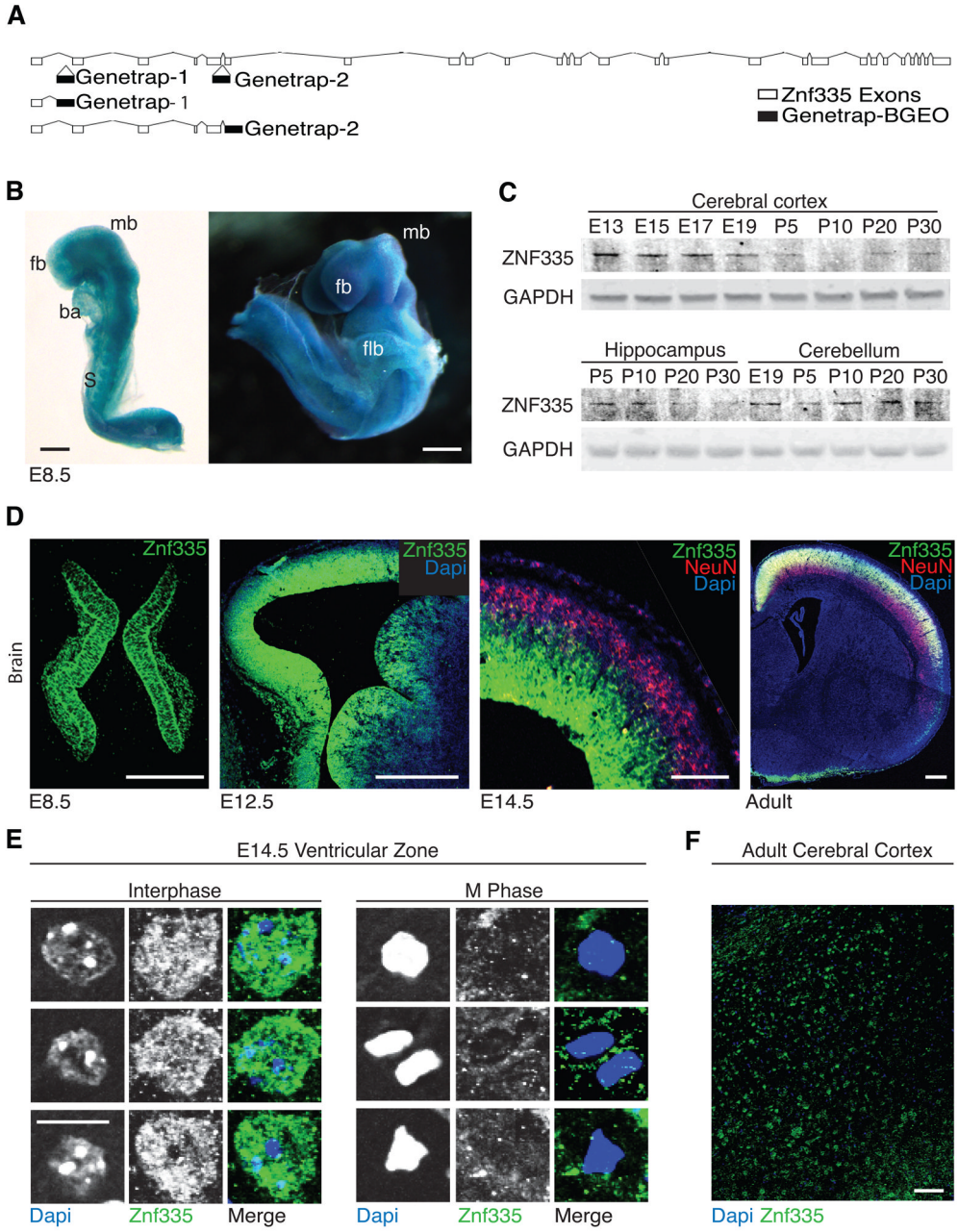

Figure 3. Znf335 is essential for mouse development and is expressed in nuclei of progenitor cells

(A) Location of genetrap insertion of two genetrap mice leading to early truncation of protein to mimic a null allele.

(B) Znf335 is expressed at E8.5 in developing forebrain (fb), midbrain (mb), somites (S), Branchial arch (ba), Forelimb bud (flb). Scale: 300μm.

(C) Western blot analysis of Znf335 protein expression throughout brain development. In the cortex, expression is highest at E13.5 before tapering off and returns slightly postnatally.

(D) Immunohistochemistry shows Znf335 expression in progenitor cells at E8.5 and in the ventricular zone of developing cortex and not in NeuN+ neurons at E12.5 and E14.5. Protein is also expressed throughout cortical plate later in development. Scale: 50, 50, 50, 400μm.

(E) Znf335 localizes to the nucleus, and colocalizes with euchromatin of progenitor cells in the ventricular zone of developing mouse brain, while Znf335 is excluded from heterochromatic foci. This colocalization disappears in cells in the M-Phase of the cell cycle. Scale: 10μm.
(F) Sparse expression of Znf335 in adult cerebral cortex. Scale: 100μm.
See also Fig S2.

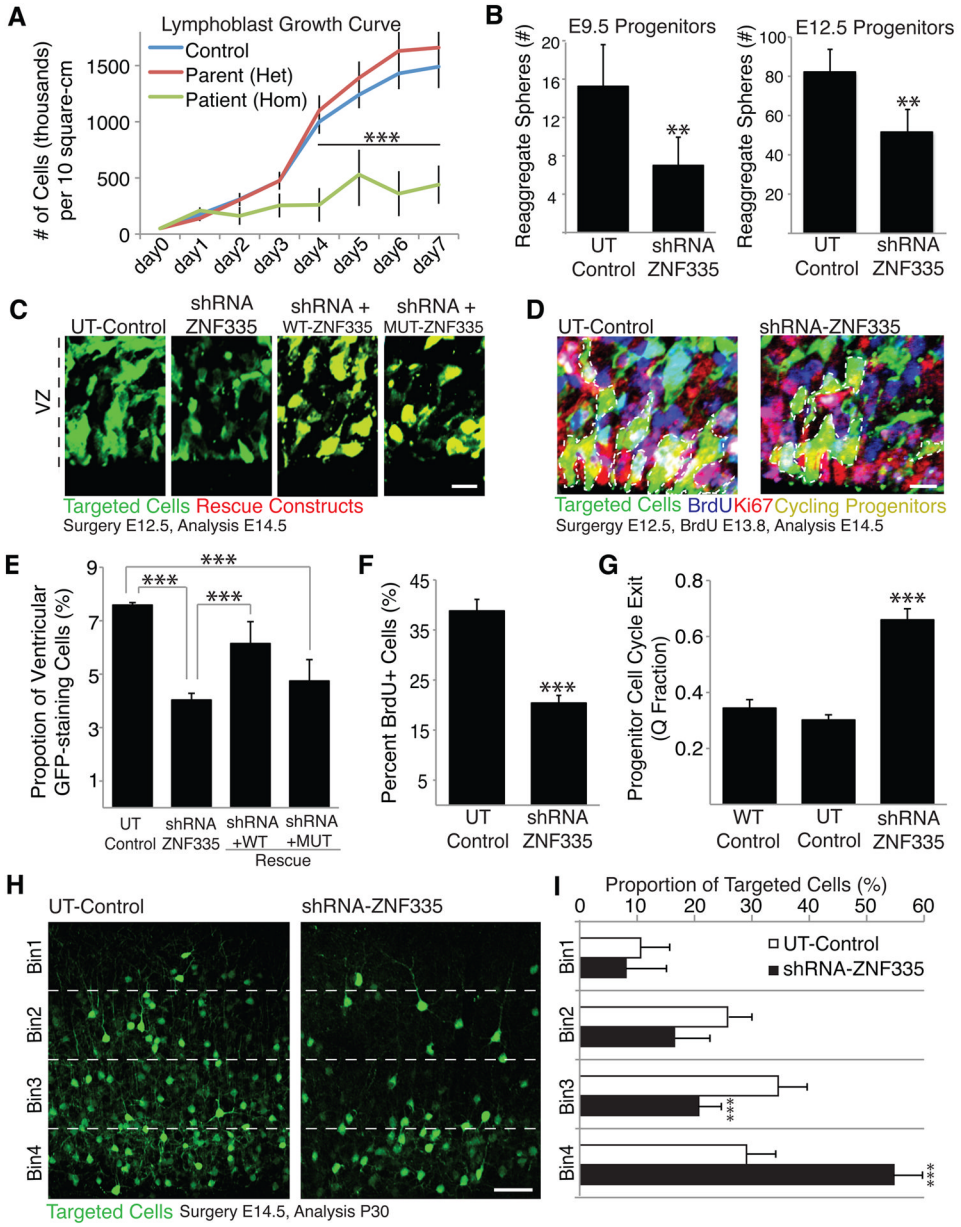

Figure 4. Znf335 is essential for progenitor cell proliferation and cell cycle maintenance

(A) Growth curves of lymphoblast cell lines derived from heterozygous parent, homozygous patient and control shows decreased growth rate in cells from patient with low levels of mutated ZNF335.

(B) Knockdown of Znf335 leads to decreased formation of progenitor cell reaggregates in E9.5 and E12.5 progenitor cell cultures showing decreased proliferation upon knockdown of Znf335. E9.5: UT-Control, 15.25 +/− 4.3; ShRNA-ZNF335, 7.1 +/−2.9, T-test, p=0.0032, n=6; E12.5 UT-Control, 82.2 +/− 11.5; ShRNA-ZNF335, 51.6+/− 11.6, Data are representated as mean +/−SD. T-Test, p=0.001; n=6 rounds of FACS sorting. Each sort is from pooled embryos from 3 different dams with roughly half of their embryos electroporated with either shRNA-Znf335 or UT-control constructs.

(C) shRNA-ZNF335 knockdown leads to fewer cells present within the ventricular zone when compared to UT-Control. WT-ZNF335 rescues the number of progenitors but MUT-ZNF335 does not. Scale: 10μm.
(D) shRNA-ZNF335 knockdown leads to fewer cycling progenitors in the ventricular zone as compared to the UT-Control. Scale: 10μm.
(E) Quantification of 4C. Knockdown of Znf335 leads to fewer percentage of targeted cells present within 250μm^2 of the ventricular zone as compared to UT-Control. WT-ZNF335 rescues the amount of GFP-staining cells in the VZ while MUT does not. UT-Control: 7.59 +/− 0.09; ShRNA-ZNF335: 4.0 +/− 0.25; shRNA+WT: 6.27 +/− 0.7; shRNA+MUT: 4.74 +/− 0.8, mean+/−SD, T-test, P=0.0001; n=12 means of different electroporated litters.
(F) Knockdown of Znf335 leads to fewer cells that are BrdU positive 48hours post knockdown within 50μm^2 of the ventricular zone as compared to UT-Control. UT-Control: 38.8 +/− 2.9; shRNA-ZNF335: 20.4 +/− 1.7, mean +/−SEM, T-test, P=0.0001; n=12 electroporated brains that were analyzed using serial sections).
(G) Knockdown of Znf335 leads to increased cell cycle exit (decreased BrdU+/Ki67+ cells out of total BrdU+ cells) as compared to UT-Control. (WT-Control: 0.34 +/− 0.03; UT-Control: 0.30 +/− 0.02; ShRNA-ZNF335: .66 +/− 0.04, mean+/−SD, ANOVA, P<0.0001; n=12 electroporated brains that were analyzed used serial sections).
(H) Knockdown of Znf335 leads to more targeted cells in the lower layers of the mouse cortex and fewer targeted cells in upper layers of the mouse cortex, indicating more premature neurogenesis upon knockdown of Znf335. Earlier born neurons reside in deeper layers vs. later born neurons that reside in the upper layers. Scale: 50μm.
(I) Cortex was divided into equal-sized bins and counted for proportion of targeted cells present in that bin. *UT-Control:* Bin1: 10.6 +/− 4.9; Bin2: 25.8 +/?− 3.7; Bin3: 34.6 +/− 5.2; Bin 4: 29.1 +/− 4.8; *shRNA-ZNF335:* Bin1: 8.1 +/− 7.1; Bin2: 16.5 +/− 6.1; Bin3: 20.7 +/− 3.6; Bin4: 54.7 +/− 5.1. mean+/−SD, T-test; Bin3:P=0.0003, Bin4:P=0.0001; n=12 electroporated brains. Only matching sections between conditions were compared.
See also Fig S3.

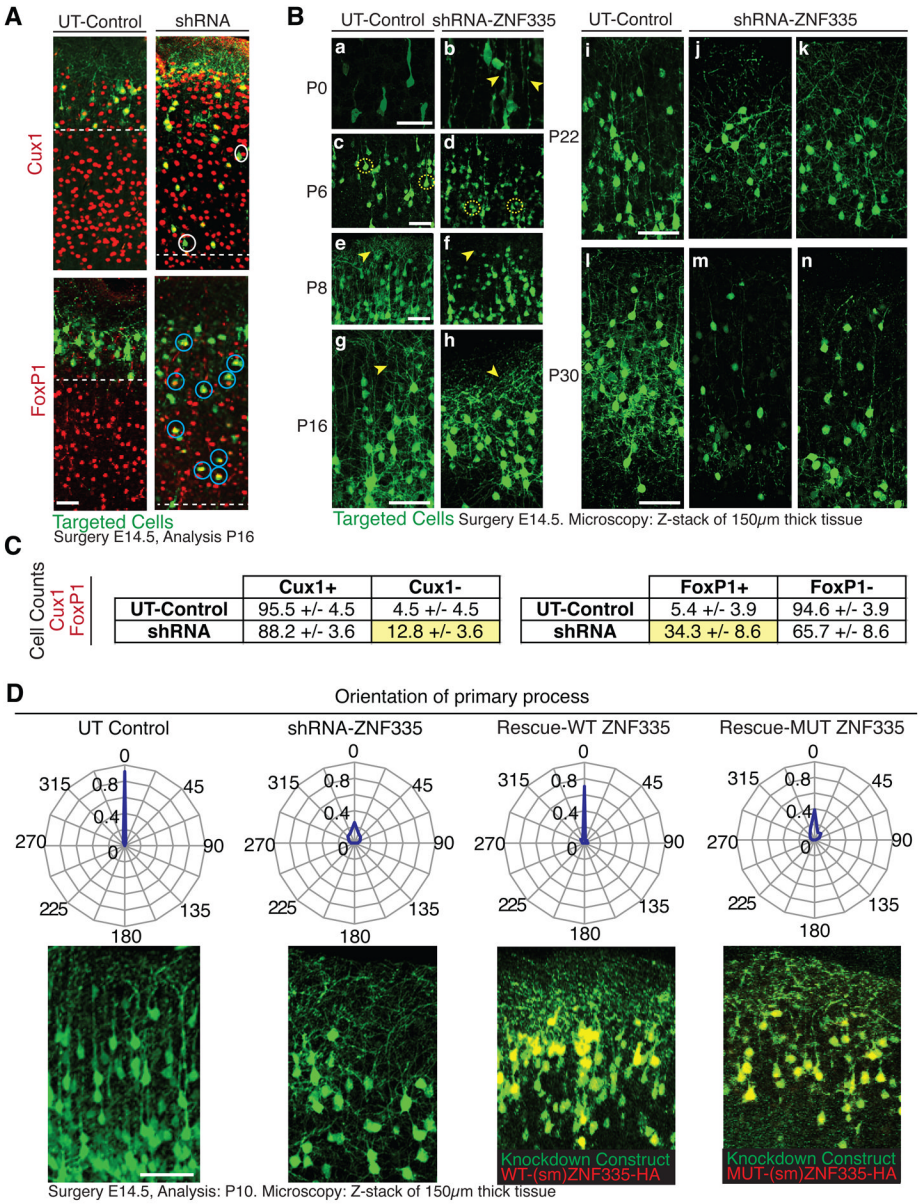

	Cux1+	Cux1-
UT-Control	95.5 +/- 4.5	4.5 +/- 4.5
shRNA	88.2 +/- 3.6	12.8 +/- 3.6

	FoxP1+	FoxP1-
UT-Control	5.4 +/- 3.9	94.6 +/- 3.9
shRNA	34.3 +/- 8.6	65.7 +/- 8.6

Figure 5. Znf335 deficiency leads to decreased cell size, and abnormal dendritic shape and orientation

(A) Knockdown of ZNF335 leads to reduction of cells in the cortical plate and production of Cux1-negative (white circles) and FoxP1-positive (blue circles) cells showing a change in cell fate. Dashed line represents end of zone containing GFP-positive cells. Scale: 50μm.

(B) Knockdown and control cells were targeted at E14.5 and analyzed at P0 (a,b), P6 (c,d) to show abnormal radial glia (P0, arrowhead) and abnormal cell body shape and size (P6, dashed circle). There is abnormal dendritic arborization (arrowhead) and orientation in knockdown cells at P8 (e,f), P16 (g,h), P22 (i,j,k), and P30 (l,m,n). Scale: 50μm.

(C) Analysis of 5A. Knockdown showed production of more Cux1-negative cells as compared to Control, and production of more FoxP1-positive cells as compared to Control.

(D). Knockdown cells show abnormal orientation based on orientation of their basal dendritic process which is normally perpendicular to the pial surface of the brain. WT-ZNF335 rescues the orientation but MUT-ZNF335 does not. Scale: 50μm. 0.92 of total UT-

Control cells have apical process orientated perpendicular to pial surface (0°), 0.03 at 22.5°, and 0.04 at 337.5°. shRNA-ZNF335 knockdown cells have only 0.25 of total cells oriented at 0°, 0.13 at 22.5°, 0.11 at 45°, 0.08 at 67.5°, 0.04 at 90°, 0.04 at 270°, 0.08 at 292.5°, 0.12 at 315°, and 0.13 at 337.5°. WT-ZNF335 rescue of shRNA-ZNF335 knockdown have 0.7 cells at 0 °, 0.03 at 22.5 °, 0.05 at 45 °, 0.3 at 67.5 °, 0.04 at 90 °, 0.02 at 270 °, 0.03 at 292.5 °, 0.07 at 315 °, and 0.05 at 337.5 °. MUT-ZNF335 rescue of shRNA-ZNF335 knockdown have 0.4 cells at 0 °, 0.1 at 22.5 °, 0.11 at 45 °, 0.06 at 67.5 °, 0.01 at 90 °, 0.03 at 270 °, 0.06 at 292.5 °, 0.08 at 315 °, and 0.14 at 337.5 °. Data presented as proportion of total cells oriented in +/−11.25 ° of radial direction n=6 electroporated brains. Only matching sections were analyzed between different conditions.
See also Fig S4.

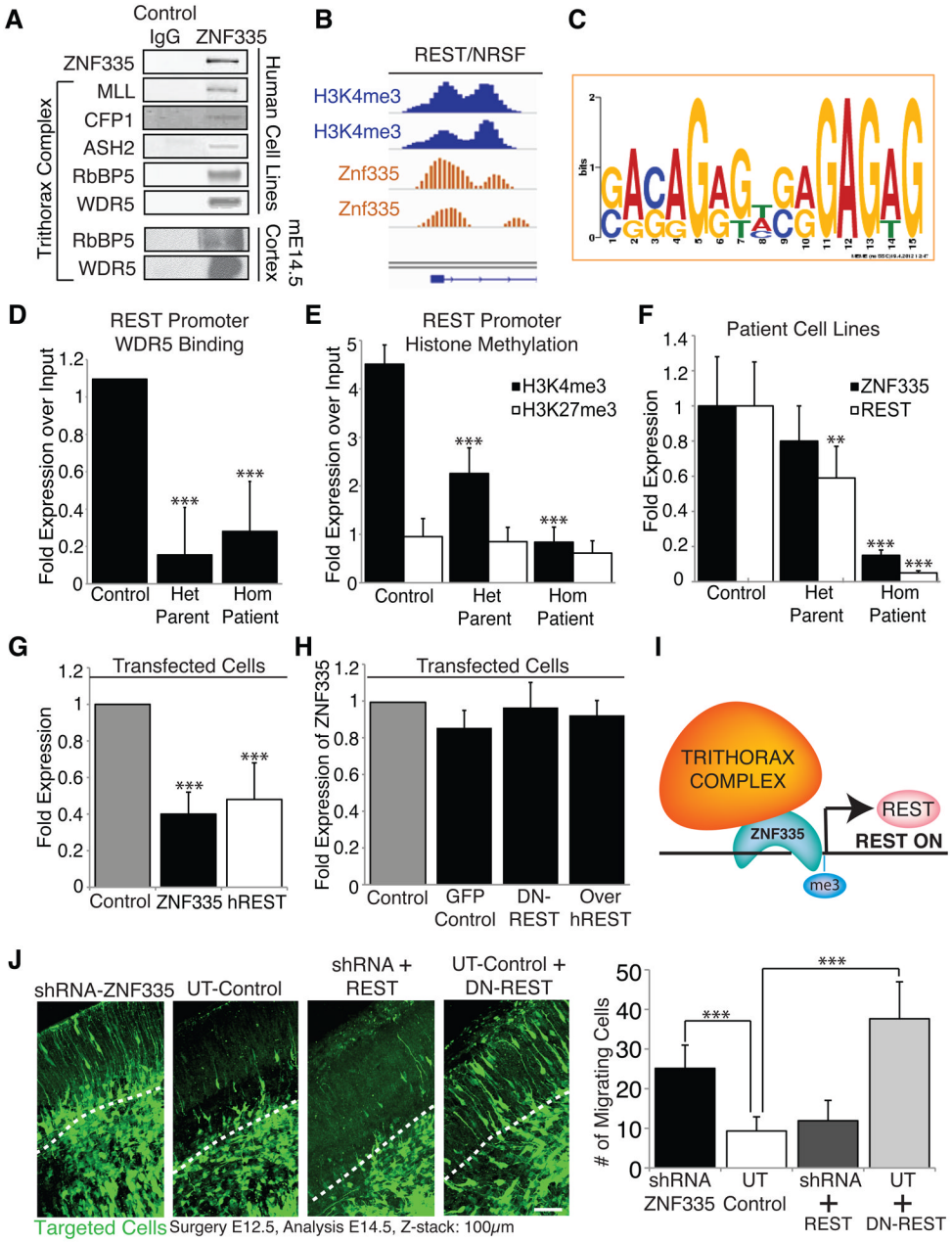

Figure 6. Znf335 interacts with trithorax complex proteins and is upstream of many neuronal differentiation genes including REST/NRSF

(A) Blots show co-immunoprecipitation of Znf335 with members of the trithorax complex in human cell lines and mouse E14.5 cortex indicating an interaction of Znf335 with the histone mehtyltransferase complex.

(B) Znf335 binds to promoter region of *REST/NRSF*, and overlaps peaks of H3K4me3 binding.

(C) Promoter Binding consensus motif for Znf335 with GAGAG motif that is predicted for C2H2 zinc fingers (Omichinski et al., 1997).

(D) Decreased binding of trithorax complex proteins such as WDR5 to the *REST* promoter under low levels of Znf335. WDR5: Control: 1.09 +/− 0, Het Parent: 0.16 +/− 0.25, Hom Patient: 0.28 +/− 0.27; chromatin was obtained and compiled from 3 different growth

cultures. Two IPs were performed for each pooled set of chromatin isolated from lymphoblast cell lines, and qPCR was run in triplicates in comparison to input. All qPCR runs were normalized to GAPDH.

(E) Decreased H3K4 trimethylation (marker of gene activation) of the *REST* promoter under low levels of Znf335, but no changes in H3K27 trimethylation. H3K4me3: Control: 4.5 +/− 0.39, Het Parent: 2.25 +/− 0.53, Hom Patient: 0.84 +/− 0.3; H3K27me3: Control: 0.95 +/− 0.37; Het Parent: 0.85 +/− 0.29; Hom Patient: 0.6, +/− 0.25; chromatin was obtained and compiled from 3 different growth cultures. Two IPs were performed for each pooled set of chromatin isolated from lymphoblast cell lines, and qPCR was run in triplicates in comparison to input. All qPCR runs were normalized to GAPDH.

(F) qPCR measurement show lower levels of properly spliced *ZNF335* expression and *hREST* expression in het parents and hom patients as compared to controls. ZNF335 analysis was done with primers specific to only the properly spliced mRNA. Incomplete splice forms would not have been picked up with primer pairs (Exon19F, Exon 20R, Exon21R): Control: 1 +/− 0.28, Het Parent: 0.80 +/− 0.21, Hom Patient: 0.15 +/− 0.03; hREST: Control: 1 +/− 0.25; Het Parent: 0.59 +/− 0.18; Hom Patient: 0.05, +/− 0.01; Mean +/−SD, T-test compared to control, homozygous patients $p<0.001$; n=9 qPCR readouts from 3 different growth cultures. RNA was extracted from lymphoblast cell lines. All qPCR runs were normalized to NMYC and GAPDH.

(G) Decreased levels of *hREST* expression is seen upon direct knockdown of ZNF335. Control: 1, ZNF335: 0.41 +/− 0.12, P=0.0001; hREST: 0.48 +/− 0.20, P=0.0001; Mean+/−SD, T-test; n=6 individual transfections of HeLa cell lines. All qPCR runs were normalized to GAPDH.

(H) Converserly, *ZNF335* expression is not significantly changed upon expression of Dominant-Negative REST, or overexpression of hREST. 6H: GFP Control: 0.85 +/− 0.09; DN-REST: 0.97 +/− 0.14; Over-hREST: 0.92 +/− 0.08; Mean+/−SD, T-test, non-significant; n=3 sets of transfections of HeLa cell lines. Similar results also seen with Hek293 cells lines (data not published). All qPCR runs were normalized to GAPDH.

(I) Schematic of Znf335 interacting with the trithorax complex to trimethylate H3K4 at the promoter of *REST* to turn on *REST* expression.

(J) Knockdown of Znf335 leads to premature cell cycle exit and neuronal migration in cortical plate. Addition of REST rescues the phenotype and recapitulates control while addition of dominant-negative REST mimics Znf335 knockdown phenotype. Dashed line represents bottom of cortical plate. Scale: 50μm. UT-Control: 9.32 +/− 3.57; shRNA-ZNF335: 25.6 +/− 8.34; shRNA+REST rescue 11.92 +/− 5.1; UT+DN-REST rescue: 37.6 +/− 0.3. UT-shRNA P=0.0001, UT-DNREST rescue P=0.0001; Mean+/−SD, T-test; n=3 different electroporation litters, and analysis from each litter was pooled. See also Fig S5 and Tables S1–S7

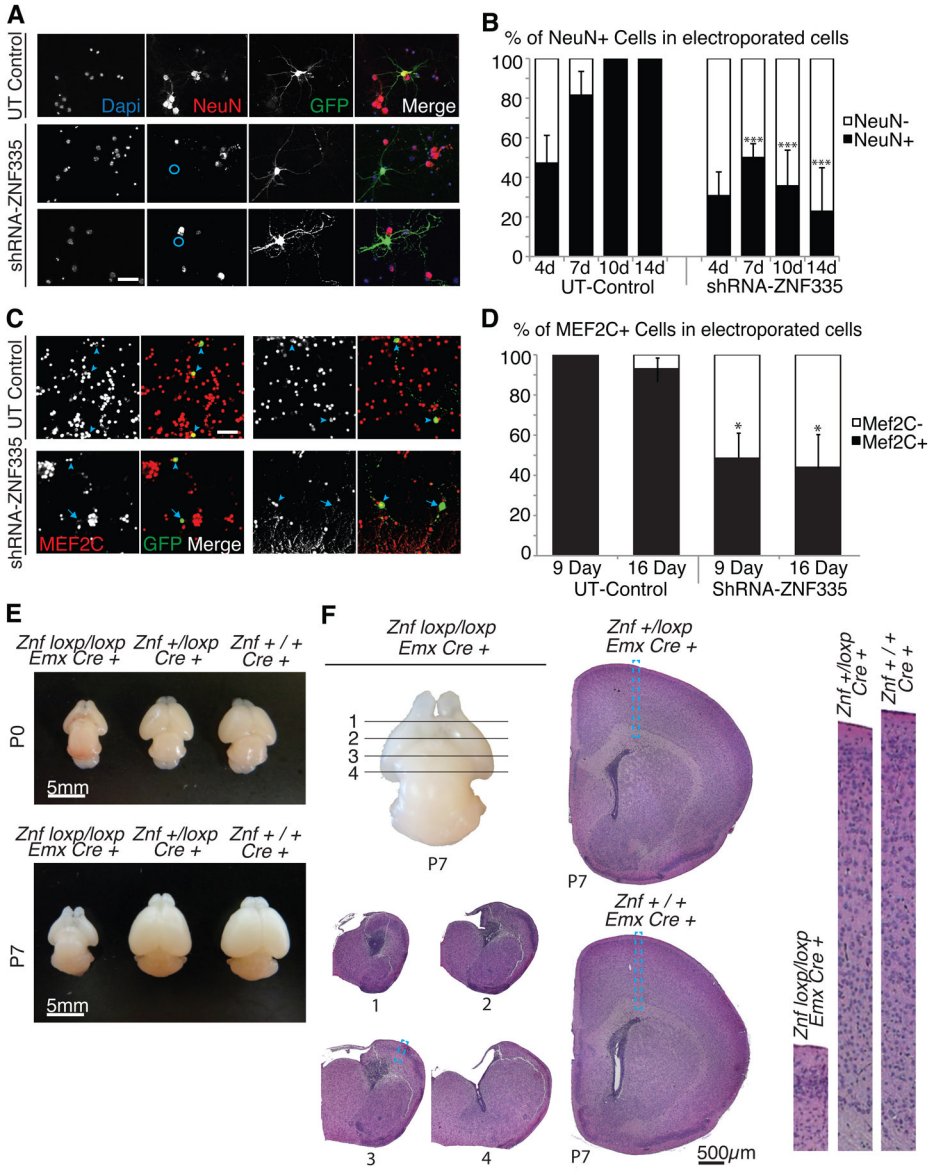

Figure 7. Znf335 is essential for neuronal differentiation and brain development

(A) Knockdown of Znf335 leads to presence of NeuN- cells (blue circles) that nonetheless have neuronal morphology in 14 day culture systems. NeuN is a marker of differentiated neurons. Scale: 20μm.

(B) Quantification of NeuN+ and NeuN- cells upon knockdown of Znf335 in short and long term culture shows decreased production of NeuN+ cells over long term culture. Control NeuN+: 4day: 48.2+/−14.1; 7day: 81.5+/−12.1; 10day: 100+/−0.9; 14day: 100+/−1.5; shRNA-ZNF335 NeuN+: 4day: 30.7+/−12.3; 7day: 50.0+/−7.0; 10day: 35.7+/−18.1; 14day: 22.9+/−19.1); Mean+/−SD, T-test, 7,10,14day: P<0.0001; n=12 separate cortical neuron cultures from 12 litters.

(C) Knockdown of Znf335 leads to Mef2C- cells (arrows), while UT Control shows Mef2C + cells (arrowhead). Scale: 20μm.

(D) Quantification of Mef2C+ and Mef2C- cells shows decreased production of Mef2C+ cells upon knockdown of Znf335 in short and long term cultures. Control Mef2C+: 9day: 100+/−0.8; 16day: 93.0+/−8.2; shRNA-ZNF335 Mef2C+: 9day: 48.5+/−12.1; 16day: 44.0+/

−15.2); Mean+/−SD, T-test, 9Day:P=0.0018, 16day:P=0.008; n=3 separate granule cell cultures from 3 different litters.

(E) Znf335 CKO (*Znfloxp/loxp;Emx1Cre+*) shows decreased formation of cerebral cortex in all areas where *Emx1-Cre* is expressed, and a small lateral cortex in areas where *Emx1-cre* is reduced or turned on later at both P0 and P7.

(F) H&E stain of coronal brain sections of ZnfCKO (*Znfloxp/loxp;Emx1Cre+*), ZnfHet (*Znf +/loxp;Emx1Cre+*), and ZnfWT (*Znf+/+;Emx1Cre+*) shows that ZnfCKO lack all cortical structure and cortical neurons. The loss of cortical brain structure leads to the formation of a small brain with a thin sheath of tissue and enlarged ventricles. Blue dashed boxed represent enlarged cortical sections (Right panels). See also Fig S6 and S7.